

3D EPID based dosimetry for pre-treatment verification of VMAT – methods and challenges

This content has been downloaded from IOPscience. Please scroll down to see the full text.

2013 J. Phys.: Conf. Ser. 444 012010

(<http://iopscience.iop.org/1742-6596/444/1/012010>)

View [the table of contents for this issue](#), or go to the [journal homepage](#) for more

Download details:

IP Address: 134.148.201.239

This content was downloaded on 01/06/2015 at 04:35

Please note that [terms and conditions apply](#).

3D EPID based dosimetry for pre-treatment verification of VMAT – methods and challenges

PB Greer

Radiation Oncology Department, Calvary Mater Newcastle, Newcastle, NSW 2298, Australia. School of Mathematical and Physical Sciences, University of Newcastle, Newcastle, NSW 2310, Australia

E-mail: peter.greer@newcastle.edu.au

Abstract. This article presents an overview of pre-treatment verification of volumetric modulated arc therapy (VMAT) with electronic portal imaging devices (EPIDs). Challenges to VMAT verification with EPIDs are discussed including EPID sag/flex during rotation, acquisition using cine-mode imaging, image artefacts during VMAT and determining the gantry angle for each image. The major methods that have been proposed to verify VMAT with EPIDs are introduced including those using or adapting commercial software systems and non-commercial implementations. Both two-dimensional and three-dimensional methods are reviewed.

1. Introduction

It is recommended that more than 50% of cancer patients receive radiation therapy treatment [1]. Therefore this therapy represents a very important frontline treatment for cancer. With the aim to deliver higher doses of radiation to the tumour and lower doses to surrounding normal tissues, the delivery and planning approaches to radiation therapy are constantly evolving. The use of intensity modulated radiation therapy (IMRT) where the radiation beam fluence is non-uniform allows for greater shaping of dose distributions within the body and hence increased sparing of normal tissues. This has traditionally been delivered using several beams at fixed linear accelerator gantry angles. The non-uniform fluence is delivered by varying the beam aperture defined by the multileaf collimator (MLC). Because IMRT is a highly complex technique and the derived fluences are non-intuitive, the accuracy of delivery is usually verified by pre-treatment dosimetric measurements. This is mandated in some countries for every patient while in others it is optional (although extensively performed). The pre-treatment dosimetric verification comprises a comparison of a measured dose with the treatment planning system calculated dose. This can be performed on a beam-by-beam basis using two-dimensional (2D) measurement or on a whole-of-treatment basis using either a 2D measured dose-plane or less commonly a three-dimensional (3D) measurement.

Although the use of a continuously rotating gantry to delivery IMRT had been proposed for some time, the commercial implementation of this method did not occur until a new method for the derivation of the gantry motion, and multileaf apertures was derived by Karl Otto [2]. He termed this technique volumetric modulated arc therapy (VMAT). His method resulted in a highly efficient IMRT plan delivery and has therefore seen dramatic uptake in recent years. VMAT is commercially available as either RapidArc™ (Varian Medical Systems, Palo Alto, CA) or VMAT (Elekta AB, Stockholm, Sweden). The method allows for continuous variation of gantry speed, dose-rate and MLC aperture



during delivery. The delivery is controlled by specifying control points at discrete gantry angles. For example for the Varian system two sets of control systems are used; 1) the fractional monitor units (MU) versus gantry angle, and 2) the MLC shape versus gantry angle. This highly complex delivery technique requires rigorous pre-treatment verification. Various existing dosimetry arrays have been utilised and in addition some new devices have been specifically designed for VMAT measurements. As with IMRT verification, the EPID represents a potentially very efficient method to verify VMAT, due to the very rapid setup time, immediate digital format, high resolution of the individual photodiodes, high level of reproducibility, and integration with the linear accelerator software. This review article outlines the major approaches that have been developed to date for the use of EPID for pre-treatment verification of VMAT and discusses some of the major challenges that must be overcome. The article is restricted in scope to verification of the recently developed VMAT technique of Otto (or similar) delivered on medical linear accelerators and recorded with two-dimensional EPID systems using non-transmission dosimetry (i.e. no phantom is present in the beam).

2. Challenges for pre-treatment dosimetric verification of VMAT with EPIDs

This section discusses some of the issues for using EPIDs for dosimetry that are specific to VMAT verification. More general issues for EPID dosimetry are covered elsewhere [3, 4].

2.1. EPID sag/flex during arc

When acquiring an integrated EPID image during gantry rotation the EPID will sag as a function of gantry angle. The effect of this is to displace the acquired frames from each other on the EPID detector with subsequent blurring of the integrated dose. Mans et al. [5] aligned single frames (typically one frame every 20 degrees) acquired during VMAT with the corresponding control point field outline. They applied the same shift to all neighbouring frames (over ± 10 degrees). They quoted the magnitude of the EPID flex as 4 mm peak-to-peak at the EPID level. Rowshanfarzad et al. [6] measured the EPID sag for the Varian system as a function of gantry angle during arc rotation using a marker placed at isocentre and corrected for the effect of the marker displacement from the mean isocentre position. They found that the sag pattern is very reproducible but is accelerator dependent. The sag was largest in the inplane direction with an amplitude of approximately 1 mm (at the isocentre level) and smaller in the crossplane direction with an amplitude of less than 0.5 mm. One accelerator was found to have a much larger amplitude of nearly 5 mm in the inplane direction. They showed that the sag degrades Gamma results in the regions of steep dose gradients. To correct the sag, they acquired cine-mode images, correcting each image according to the previously derived sag map values at that gantry angle, and then recombined the images to form an integrated image. This approach was limited to shifting each image to the nearest pixel. Other authors have also measured the EPID sag [7, 8]. An entirely different approach was developed by Iori et al. who used an additional holding device which clamped to the accessory mount and held the EPID in position during rotation [9]. They were able to restrict the EPID sag to less than 1 mm with this device. The EPID in this case was mounted on an R-Arm which exhibits greater sag with gantry angle than the newer E-Arm.

2.2. Cine-mode imaging

For fixed beam IMRT, integrated mode EPID images are used for each beam, as the gantry angle can easily be verified visually. However for VMAT delivery, to fully verify accurate dose delivery requires that the dose is verified as a function of gantry angle. Therefore an integrated image acquired for the entire delivery would not fully validate the delivery as it compresses dose from all gantry angles into one image. This has prompted the use of cine-mode image acquisition where separate images are continuously acquired during the delivery, and these are associated with a gantry angle. For the Elekta system Mans et al. [5] modified in-house developed acquisition software to save every detector frame during imaging (~ 2.5 frames per second). For the Varian system the cine acquisition mode was not intended for dosimetry. Piermattei et al. [10] investigated cine-mode for the IAS2 system with a 0.6 Hz imaging rate. They used a low dose-rate of 100 MU/min and found good stability

(within 1%, 2 SD) of the EPID signal for this mode using weekly measurements over a three month interval in both static and dynamic conformal arc modes. They also determined that signal reproducibility within each session and signal linearity were within 1% (2 SD). McCurdy and Greer [11] investigated the dosimetric performance of the IAS3 system cine-mode (7.5 Hz) compared to integrated mode. They found that the time-resolved signal agreed well with time-resolved ion-chamber measurements but that the mode under-responded to small dose levels. This is due to the two frames that contain partial signal at beam-on being discarded with this mode (Figure 1). Similarly the two partial frames at beam-off are also discarded. This was recently confirmed using a separate frame-grabber system to acquire all frames during cine-mode acquisition of a sliding window IMRT delivery. By comparing the first frame of the cine-mode acquired data with the separately acquired frames, the discarded frames were identified. These partial frames are included with integrated mode, (although recent investigations suggest that the very last partial frame in integrated mode is still discarded). Another problem with this type of imaging is that large numbers of images can be acquired for a single VMAT delivery. This can cause memory overflow problems during delivery.

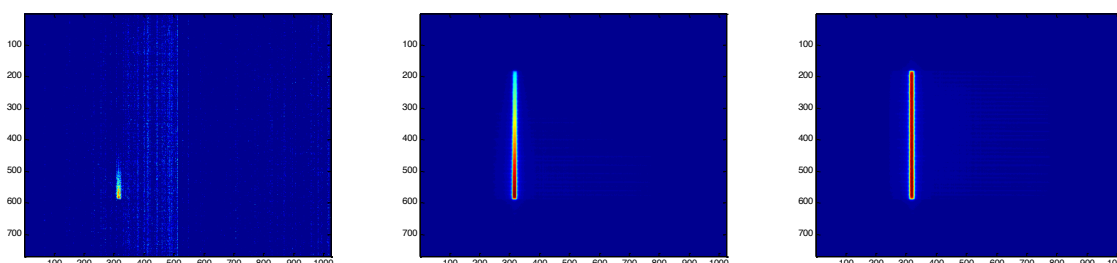


Figure 1: The first three frames acquired for a sliding window irradiation. The first two frames contain partial dose information as the beam-on occurred during the frame integration period. In the current Varian cine-mode implementation these first two frames (along with the final two partial frames that are read-out after beam-off) are discarded and some dose information is lost.

2.3. Image artefacts

For the Elekta system Mans et al. [5] reported image artefacts when they acquired individual frames using their in-house system and these were attributed to changes between discrete dose-rate levels during acquisition. This prevented them from determining the patient transmission factor using images acquired with and without the patient present, therefore they replaced this with a calculated transmission factor. For Varian systems VMAT is delivered using the pulse-drop servo to control the dose-rate (for fixed beam IMRT a pulse-length servo is used). This results in pulse-dropping artefacts in the frames of images acquired during VMAT delivery. These occur because different rows of the imager are read out at slightly different times. Therefore the time periods over which each row has integrated the dose are different. Each row can therefore integrate different numbers of beam pulses depending on when the pulses are dropped, with resulting different output signals. As the rows are read-out in batches, with each batch read-out very rapidly (virtually simultaneously), the result is banding artefacts where each batch of rows has integrated over a different number of pulses (Figure 2). These are not actual artefacts, the imager is accurately integrating the dose or pulses received, however these bands are problematic for dosimetry with cine-images as the non-uniform dose delivery is not included in any modelling or treatment planning system reference dose. The simplest method to reduce this is to average multiple frames for each cine image. However this has the disadvantage of averaging dose delivery over an increasing range of gantry motion. Further methods to account for these artefacts should be investigated.

2.4. Gantry angle for each cine-image

Methods are required to associate a gantry angle to each cine-image. Mans et al. [5] using their in-house acquisition software recorded the gantry angle via an iCom connection to the treatment machine

and stored this with every recorded image frame. They investigated the lag of this gantry angle using a dedicated phantom with imbedded steel ball-bearings (BB's) to obtain the gantry angle from the image of the phantom. Their analysis found a lag of ~ 0.4 s or about one frame for the gantry angle. To compensate for this they used the average gantry angle of the acquired frame and the two successive frames. For a Varian C-Series linear accelerator the accuracy of the gantry angle stored in the DICOM image header was investigated by Ansbacher et al. [12] using a custom-designed "radiographic inclinometer" phantom. The phantom consisted of a pair of lead solder wires spiralled along the surface of a 20 cm long acrylic tube. As the gantry rotates the apparent intersection point of the wires moves proportionally along the axis of the tube. From the length of the intersection point the gantry angle range for each cine-image could also be measured. By comparing the imaged gantry angle and the header gantry angle they found that the header angle lagged the imaged angle for 3 frame averaged cine-images and from the number of repeated angle instances they suggested that the angle is updated no more than 2-3 times per second. The header angle accuracy was also investigated by McCowan et al. by comparison to dynalog file data, a separate encoder, and a similar radiographic inclinometer [13]. They found that the header angle can have errors of several degrees. Adamson and Wu [14] also determined the accuracy of the header angle as 1.0 ± 0.8 degrees although the reference angle source was not stated. At present to associate an accurate gantry angle with the EPID image requires the use of an external angle source which must be synchronised with the EPID images. The Varian TrueBeamTM accelerator uses an accurate encoder to populate the header with the gantry angle [D. Morf, Varian Medical Systems, private communication].

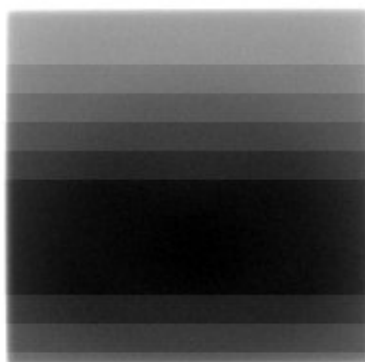


Figure 2: Example cine-mode frame of an open field illustrating the banding artefacts due to pulse-dropping during the acquisition.

3. Methods for pre-treatment dosimetric verification of VMAT with EPIDs- 2D

3.1. Commercial software systems

The Varian Portal DosimetryTM system was developed for the pre-treatment verification of IMRT and has become widely used at many centres. The system has a model that uses details of the treatment plan to derive a prediction of the EPID response for the IMRT beam [15]. The model is very simple, a "fluence" matrix is first derived which represents the relative beam-on fraction. This is convolved with a triple-Gaussian kernel to model the dose-deposition in the EPID. A field-size dependent correction factor is applied which is derived by comparison of predicted and measured EPID response for a range of jaw-defined fields. The EPID response is calibrated to CU units by delivering a 10×10 cm² field of 100 monitor units to the EPID, and specifying a CU value. The prediction model then scales its data to CU so that the prediction and measurement can be compared in absolute CU units without normalisation. EPID images are acquired in integrated mode which collects image frames during the entire delivery and then stores an integrated CU value.

Iori et al. [9] have investigated the application of this system to VMAT verification for 23 fields. They stabilised the EPID detector using an ancillary holding device clamped to the accessory mount which holds the EPID in place during gantry rotation. As the prediction model required an IMRT plan, they used an “IMAT-SIM” converter to translate the VMAT delivery into a static gantry angle IMRT field plan. The Portal Dosimetry system was then able to predict the EPID image for this IMRT plan. The delivery at the linear accelerator was performed using both static gantry IMRT and VMAT. They found that the percentage of field-area that failed Gamma analysis with criteria of 3% and 3 mm was $3.0\% \pm 3.6\%$ (mean \pm 1 SD) for IMRT delivery and $3.4\% \pm 3.9\%$ for the VMAT deliveries. A higher tolerance of 5% for the dose-difference was used for outer x-ray beam regions. The correlation between the fail rates for the IMRT and VMAT deliveries was within 1%.

The GLAaS algorithm converts measured EPID images to a dose-in-water plane [16]. These can then be compared to treatment planning system dose to water calculations for the IMRT beam. It does this by approximating the IMRT delivery as a series of N static segments and deriving correction factors that are applied to the EPID image based on an equivalent field size of each segment (termed equivalent window width Field ewwF). Empirically derived look-up tables are generated that relate EPID response to dose-in-water as a function of ewwF and depth in water. It also accounts for the difference in response of the EPID to open and MLC transmitted components of the delivered segment. Nicolini et al. [8] applied this method to VMAT plans delivered on Varian systems. They tested seven clinical-type deliveries using integrated images acquired over entire (360 degree) arcs. The EPID-derived dose-in-water was compared to Eclipse treatment planning system calculations where the VMAT delivery was collapsed onto an infinitesimally small gantry rotation, generating the integrated dose distribution for the entire arc on a single dose plane. Every control point was individually calculated and accumulated. They obtained Gamma pass rates with 3%, 3 mm criteria of $97.7 \pm 1.2\%$ (mean \pm 1 SD) at 6 MV and $94.9 \pm 1.3\%$ at 18 MV. Some preliminary tests with shorter partial arcs of 6 or 12 degrees were also performed. For two plans, three consecutive partial-arcs were delivered and measured with the EPID. In these cases separate plans in Eclipse were generated encompassing the control-points corresponding to the arc. For the 6 degree arcs this comprised 4 control points (including start and stop points) with each control point representing 2 degrees of rotation. Tests of the short arcs were performed on a simplified VMAT implementation with constant dose-rate and gantry speed. Gamma analysis results were above 96.0% pass-rate with 3%, 3 mm criteria. In a much larger study from the same group a total of 275 patients with 375 arcs were examined [17]. The Gamma analysis results were $97.1 \pm 2.4\%$ (mean \pm 1 SD) for a 3%, 3 mm criteria.

More recently Bailey et al. [18] investigated the EPID dosimetry algorithm EPIDose (Sun Nuclear Corporation, Melbourne, FL, USA) for 26 VMAT deliveries. The EPIDose algorithm [19] converts the EPID image to a dose plane in water for direct comparison to the treatment planning system calculation. The method uses the MLC plan data and for each MLC segment shape derives a correction for the difference in EPID output factor to dose in water output factor. It also derives a correction for the difference in EPID response to open and MLC shielded portions of the segment. The EPID image is then convolved with a kernel to account for the difference in dose-deposition kernels of the EPID and water. Integrated mode EPID images were acquired for the deliveries, and the converted EPID data were compared to Eclipse calculated dose-planes. The Gamma evaluation results for 14 prostate fields was $98.2 \pm 1.7\%$ (mean \pm 1 SD) with 3%, 3 mm criteria, and for 12 head and neck fields $95.3 \pm 5.9\%$. Very similar results were obtained with a MapCheck device replacing the EPID measurements.

3.2. Other proposed methods

A non-dosimetric method has been developed by Bakhtiari et al [7]. In this method the MLC aperture is extracted from cine-mode EPID images acquired during VMAT delivery. These apertures are compared to the apertures defined in the MLC delivery file, which contains the MLC apertures for each of 177 control points (gantry angles). Using the gantry angle information in the EPID image

header, the delivery file apertures were interpolated and then compared to the EPID measured aperture for that gantry angle.

4. Methods for pre-treatment dosimetric verification of VMAT with EPIDs- 3D

True 3D dosimetry with current EPIDs is not possible, as the EPIDs are inherently two-dimensional and are mounted on a support-arm. Three-dimensional dosimetry with EPIDs takes the approach of dose estimation (often termed reconstruction) in 3D within a virtual phantom or patient model calculated from the “in-air” EPID 2D measurement. A three-dimensional method to reconstruct dose in a patient model from EPID measured cine-mode transit dose images during treatment has been reported by Mans et al. [5] however this method is outside of the scope of this review. Ansbacher et al. [12, 20] have presented a method where a three-dimensional dose distribution is reconstructed in a virtual cylindrical phantom based on in-air cine-EPID measurements without any phantom present. This allows for direct comparison with an Eclipse dose calculation in a phantom with the same geometry. They compared a VMAT plan with the EPID reconstruction where every 10 EPID frames were combined into a single image before reconstructing the dose. Using a Chi 3-D comparison they found pass-rates of 84% for a high dose region (dose above 80% of the prescription) and 96% for a low dose region (dose 40-80% of prescription). By delivering the same plan as a conformal arc they were able to show that the Chi rates were markedly reduced to 55-57% with this method, however when these plans were “collapsed” onto one gantry angle the dose distributions were not able to be differentiated. This demonstrated the superior ability of gantry-angle resolved dosimetry to detect delivery errors for VMAT.

Another concept that has been recently reported in abstract form, has three-dimensional aspects in its approach [14]. The method used cine-EPID images acquired during delivery. The plan is modified so that the two most inferior MLC leaf pairs are open at all control points, and the collimator angle is zero or 90 degrees. A custom-built phantom is positioned so that it is visible on all images through the opened leaf pairs. This is used to measure the angular fraction through which each portal image is acquired. The expected values of delivered monitor units and the MLC positions at the beginning and end of each image are then derived from the angular increment. These are then used to derive a predicted detector response for this angular fraction using the Varian Portal Dosimetry prediction model outlined above. The two data sets are then separately stacked into a cube format with each image forming an x-y plane, with the z-coordinate representing the gantry angle. Each image has a leaf-motion axis and a cross-leaf axis. A projection through the data stack onto 3 planes is then formed by integrating along rays through the pixel data in the stack. The three data planes that are formed represent: leaf motion axis versus cross leaf axis; leaf motion axis versus gantry angle and cross leaf axis versus gantry angle. The 3 data planes for the measured and predicted data sets can then be compared.

5. Summary

VMAT is a highly complex delivery technique that requires careful and rigorous pre-treatment quality assurance. Ideally this quality assurance should verify the correct operation of the linear accelerator control systems for VMAT delivery, i.e. that the correct fractional MU is delivered between each gantry angle control-point and the correct MLC movement occurs between each control point. Current methods to perform pre-treatment VMAT quality assurance with EPIDs mostly do not fully realise this level of assurance, and they are predominantly 2D. Further research is required to provide more comprehensive and efficient pre-treatment quality assurance methods with EPIDs.

6. Acknowledgements

The author gratefully acknowledges the contributions of Pejman Rowshanfarzad, Brian King, Todsaporn Fuangrod, Henry Woodruff, and Michael Barnes at the Calvary Mater Newcastle. Boyd McCurdy and Peter McCowan at CancerCare Manitoba are also acknowledged for their many contributions. The author acknowledges the assistance of Daniel Morf and Varian Medical Systems

iLab, Baden, Switzerland for assistance with technical queries on image acquisition and for the loan of the frame-grabber system used to investigate cine-mode acquisition.

7. References

- [1] Delaney G *et al* 2005 *Cancer* **104** 1129-37
- [2] Otto K 2008 *Med. Phys.* **35** 310-7
- [3] van Elmpt W *et al* 2008 *Radiother. Oncol.* **88** 289-309
- [4] Greer P B and Vial P 2011 *Concepts and Trends in Medical Radiation Dosimetry*, ed A B Rosenfeld, *et al.* pp 129-44
- [5] Mans A *et al* 2010 *3D Radiother. Oncol.* **94** 181-7
- [6] Rowshanfarzad P *et al* 2012 *Med. Phys.* **39** 623-35
- [7] Bakhtiari M *et al* 2011 *Med. Phys.* **38** 1366-73
- [8] Nicolini G *et al* 2008 *Radiat. Oncol.* **3**
- [9] Iori M *et al* 2010 *Med. Phys.* **37** 377-90
- [10] Piermattei A *et al* 2009 *Med Biol Eng Comput* **47** 425-33
- [11] McCurdy B M C and Greer P B 2009 *Med. Phys.* **36** 3028-39
- [12] Ansbacher W *et al* 2010 *J. Phys.: Conf. Ser.* **250** 108-11
- [13] McCowan P M *et al* 2011 *Med. Phys.* **38** 3534
- [14] Adamson J and Wu Q 2012 *Phys. Med. Biol.* **57** 6587-600
- [15] Van Esch A *et al* 2004 *Radiother. Oncol.* **71** 223-34
- [16] Nicolini G *et al* 2006 *Med. Phys.* **33** 2839-51
- [17] Fogliata A *et al* 2011 *Br. J. Radiol.* **84** 534-45
- [18] Bailey D W *et al* 2012 *J. Appl. Clin. Med. Phys.* **13** 82-99
- [19] Nelms B E *et al* 2010 *J. Appl. Clin. Med. Phys.* **11** 140-57
- [20] Ansbacher W *et al* 2006 *Med. Phys.* **33** 3369-82